JOURNAL OF MATERIALS SCIENCE: MATERIALS IN MEDICINE 13 (2002) 1123–1127

Structural analysis of Si-substituted hydroxyapatite: zeta potential and X-ray photoelectron spectroscopy

C. M. BOTELHO[1], M. A. LOPES[1,2], I. R. GIBSON[3], S. M. BEST[4], J. D. SANTOS[1,2*]
[1]*INEB – Instituto de Engenharia Biomédica, Rua do Campo Alegre, 823, 4150-180 Porto, Portugal*
[2]*Departamento de Engenharia de Metalúrgica e Materiais, Faculdade de Engenharia, Universidade do Porto, Rua Roberto Frias, 4200-465 Porto, Portugal*
[3]*Department of Biomedical Sciences, Institute of Medical Sciences, University of Aberdeen, Foresterhill, Aberdeen, AB25 2ZD, UK*
[4]*Department of Materials Science and Metallurgy, University of Cambridge, Pembroke Street, Cambridge, CB2 3QZ, UK, and St John's College, Cambridge, CB2 1TP, UK*
E-mail: jdsantos@fe.up.pt

The aim of this study was to determine the effect of the incorporation of silicon on the surface charge of hydroxyapatite (HA) and to assess surface structural changes of HA and Si–HA induced by dissolution in both static and dynamic systems. X-ray photoelectron spectroscopy (XPS) analysis showed that SiO_4^{4-} groups were substituted for PO_4^{3-} groups in the silicon-hydroxyapatite (Si–HA) lattice according to a previously proposed substitution mechanism without the formation of other crystalline phases, such as tricalcium phosphate or calcium oxide. The substituted silicon induced a decrease in the net surface charge and the isoelectric point of HA as determined by zeta potential (ZP) measurements. At physiological pH = 7.4 the surface charge of Si–HA was significantly lowered compared to unmodified HA, i.e. -50 ± 5 to -71 ± 5 eV, caused by the presence of silicate groups in the HA lattice, which may account for a faster *in vitro* apatite formation using SBF testing. XPS results indicated that silicon seems to be preferentially leached out from Si–HA surface compared to other ionic species after dissolution studies in tris-buffer using a dynamic system.

Introduction

In the 1970s several groups demonstrated that bone mineralization requires a minimum concentration of soluble silicon [1–4] and Voronkov suggested that gene activation by silicon may be due to the presence of Si–O bonds within the DNA and RNA and he concluded that silicon is an inherent component of nucleic acids where it substitutes P^{5+} [5]. Hench reported that the deterioration in the proliferation and function of osteoblasts due to osteopenia and osteoporosis are related with the loss of biologically available silicon [6] and according to Keeting bone cells in culture proliferate more rapidly in the presence of soluble silicon [7]. These studies clearly demonstrate the enormous advantage of the incorporation of silicon in the biomaterials lattice aimed at regenerating bone tissue.

Specifically related to the biomaterials field, glasses, and glass-ceramics with SiO_2-based components have been developed and are now being used in several clinical applications [8]. When these materials are introduced in physiological solutions the reactions involving the silicate groups are very rapid, which enhances the bioactivity of materials [9] leading to the formation of an apatite layer on the surface. *In vivo* a similar layer is also observed at the bone/implant interface [10].

In order to take advantage of the positive biological effect of silicon a new bioceramic has been developed, Si-substituted hydroxyapatite (Si–HA), using a chemical precipitation route [11, 12]. Previous studies have shown that the silicon substitution resulted in enhanced cell activity *in vitro* [13] and increased bone apposition/ingrowth *in vivo* [14] relative to stoichiometric hydroxyapatite.

It is well known that surface charge plays an important role in the cell adhesion process [15–17]. Cells adhere on both positively and negatively charged surfaces but the morphology of adhering cells may vary depending on the sign of the electrical charge [17, 18]. Numerous studies have demonstrated that the surface structure and composition of bioceramics influence their cytocompat-

*Author to whom all correspondence should be addressed.

ibility and affect the sequence of steps that lead to bone bonding [19–24].

The aim of this study was to determine the effect of the incorporation of silicon on the surface charge of HA and to assess surface structural changes of HA and Si–HA induced by dissolution testing performed in a SOTAX-Flow through dissolution system. Surface charge was calculated by electrophoretic mobility and surface analysis by Fourier transform infra-red spectroscopy (FTIR) and X-ray photoelectron spectroscopy (XPS).

Materials and methods

The preparation of the Si–HA was done using a precipitation chemical route and is fully described elsewhere [11, 12]. Sintered powders of the HA and Si–HA materials were prepared by compacting the as-precipitated powders and sintering them at 1300 °C and then grinding/milling the sintered specimens to form a fine powder. Powders with a specific granule size (between 20 and 53 μm) were selected for use in this study by sieving in a variety of sieve sizes.

To determine the phase purity of the precipitated material used in this study X-ray diffraction (XRD) was performed using a Siemens D5000 X-ray diffractometer. Data were collected between 25 and 40° 2θ using a step size of 0.02° and a count time of 2.5 s. Phase identification was carried out by comparing the peak positions of the diffraction patterns with ICDD (JCPDS) standards. The X-ray fluorescence confirmed the incorporation of 0.8 wt % Si and 1.2 wt % Si in the HA lattice using a Philips PW1606 spectrometer. Surface charge was measured in 10^{-4} M KNO_3 solution in a Zeta meter 3.0+ System at different values of pH ranging from 3 to 10, according to Smoluchowki's equation:

$$ZP = \frac{4\pi \times \eta}{D} \times EM \qquad (1)$$

where η, D, and EM are the viscosity (poise), the dielectric constant of the suspending liquid, and the electrophoretic mobility, respectively.

The dissolution of HA and Si–HA in a static system was assessed, whereby sintered samples were soaked in a simulated body fluid (SBF K-9). In addition to studying the dissolution in a static environment, this test would distinguish between the ability of an apatite layer to form on a HA and a Si–HA surface. Polished dense (98% of the theoretical density of HA) discs were placed into 20 ml of SBF K-9 solution and incubated at 37 °C and pH = 7.4 for periods of time between 0 and 28 days. After each time point, the Ca^{2+} and PO_4^{3-} ion concentration of the SBF solution was measured using inductively coupled plasma-emission spectrometry, ICP-ES (Department of Geology, Imperial College, London).

As an alternative to the static dissolution experiment a dynamic dissolution test was performed in a flow through dissolution system (Sotax CE6, a fraction collector Sotax C-160) in a Tris-hydroxymethyl amino-methane buffer solution at 37 °C and pH = 7.4 using a flow rate of 5.0 ml/min.

The HA and Si–HA powders were analyzed by XPS and FTIR before and after the dynamic dissolution test.

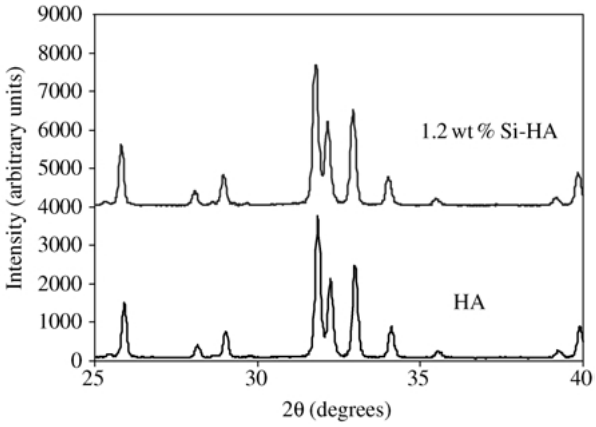

Figure 1 X-ray diffraction patterns for HA and Si–HA.

In the XPS analyses Mg-Kα was used as the radiation source and spectra referred to adventitious carbon at 285.0 eV. A Gaussian–Lorentzian function was applied for fitting the spectra using the XPSPEAK Version 4.0 software. FTIR spectra were obtained using a System 2000 FT-IR/NIR FT-Raman with a resolution of 4 cm^{-1} and by averaging 100 scans.

Results

The XRD patterns of the HA and 1.2 wt % Si–HA sintered powders are presented in Fig. 1. The substitution of silicon into the HA lattice did not affect the phase composition, as no secondary phases, such as tricalcium phosphate or calcium oxide, were formed.

Fig. 2 shows the FTIR spectra of HA and Si–HA. In the spectrum of HA it is possible to observe the peaks that correspond to PO_4^{3-} groups: 1089, 1046, 958, 600, and 569 cm^{-1} and to the OH^- group, 3570 and 630 cm^{-1}, whose wavelengths are in accordance with literature values [25]. For the 1.2 wt % Si–HA, two additional peaks were detected at 888 and 504 cm^{-1} that can be assigned to the SiO_4^{4-} group [26]. It is also worth noting that the peak that corresponds to the OH^- group at 630 cm^{-1} underwent a significant decrease in intensity with the introduction of silicon into the HA lattice.

The results in Fig. 3 show that the isoelectric point of HA was at a pH ≈ 5.5 and with the substitution of 0.8 wt % of silicon into the HA, a shift was observed

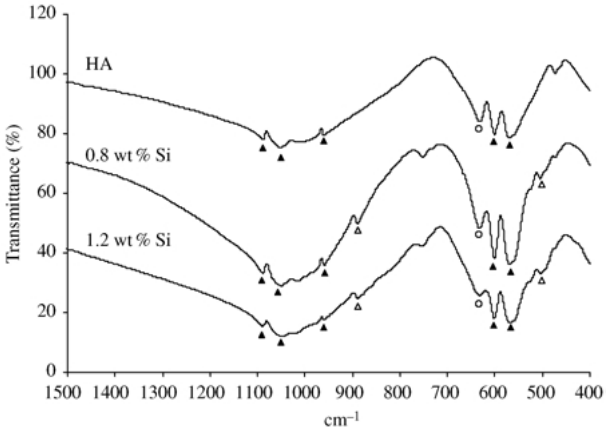

Figure 2 FTIR spectra of HA, 0.8 wt % Si–HA and 1.2 wt % Si–HA.

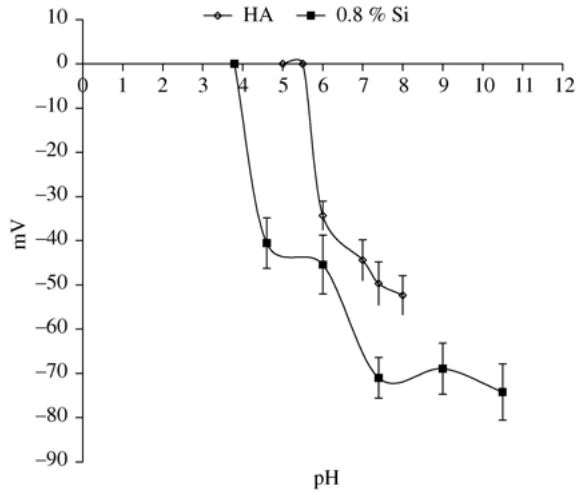

Figure 3 Zeta potential values of HA and 0.8 wt % Si–HA.

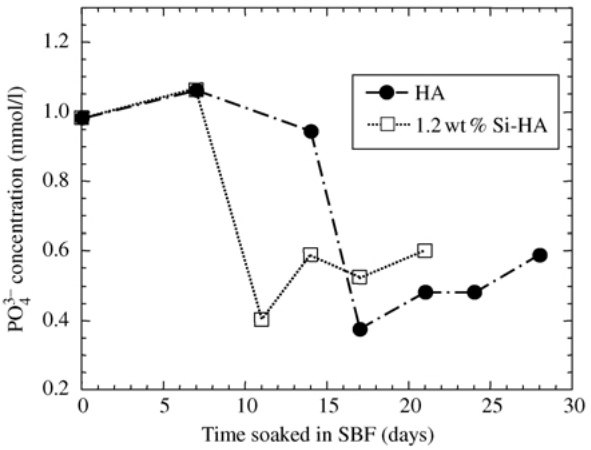

Figure 5 Phosphorous ion concentration (mmol/l) in SBF soaking solution solution.

toward a lower pH ≈ 3.8. Another interesting observation was that at a physiological pH = 7.4 ± 0.1 the zeta potential of HA was −50 ± 5 eV, whereas the zeta potential for 0.8 wt % Si was −71 ± 5 eV. Therefore, a significant shift to more negative values as a result of silicon substitution was observed.

Soaking HA and 1.2 wt % Si–HA samples in a simulated body fluid for periods of up to 28 days showed two different results. First, at the first time point (7 days) both the HA and the Si–HA behaved similarly, showing an increase in the calcium and phosphate ion content of the SBF solution, which corresponded to dissolution of these ions from the test specimens (Figs. 4 and 5). It should be noted that the increase in the Ca^{2+} ion content (approximately 0.3 mmol/l) was significantly greater than the increase in the PO_4^{3-} ion content (0.05 mmol/l). Second, the Si–HA sample resulted in a rapid decrease in the ion concentration of the SBF after 7 days, whereas the same behavior in the HA sample appeared to be delayed by several days. This decrease in the calcium and phosphate ion concentration corresponded to the precipitation of an apatite phase from the SBF solution on to the surface of the test specimens, as confirmed by SEM (data not shown). Although the HA sample initially resulted in the continued dissolution of calcium ions after 7 days, it is interesting to note that when the behavior of both materials changed from dissolution to precipitation/apatite layer formation, the decrease in the calcium and phosphate ion contents was approximately 1 and 0.6 mmol/l, respectively. The Ca/P molar ratio of this decrease corresponds to approximately 1.66, which correlates to a hydroxyapatite-like phase being formed from the solution.

Comparing the FTIR spectra of HA before and after dissolution showed that no significant change occurred. For Si–HA, however, a decrease in the peak intensities that correspond to the most important groups (SiO_4^{4-}, OH^- and PO_4^{3-}) was observed.

The FTIR results were complemented with XPS analysis of the surface of samples before and after dynamic dissolution testing, and although only small changes in the atomic percentage of Ca^{2+}, P^{5+}, and O^{2-} could be quantified after dissolution (see Table I), the Si^{5+} showed a decrease after dissolution, indicating preferential release. From Fig. 6, which shows the silicon peak detected in the Si–HA, the binding energy at 101 eV corresponds to (Si–O) bonding [27].

TABLE I Relative atomic percentages of Ca, P, O, and Si elements before (b) and after (a) dynamic dissolution testing

	Ca	P	O	Si
HA – b	23.31	16.60	60.09	—
HA – a	23.03	17.58	59.39	—
1.2 wt % Si–HA – b	23.46	15.98	59.28	1.28
1.2 wt % Si–HA – a	22.71	15.85	60.42	1.02

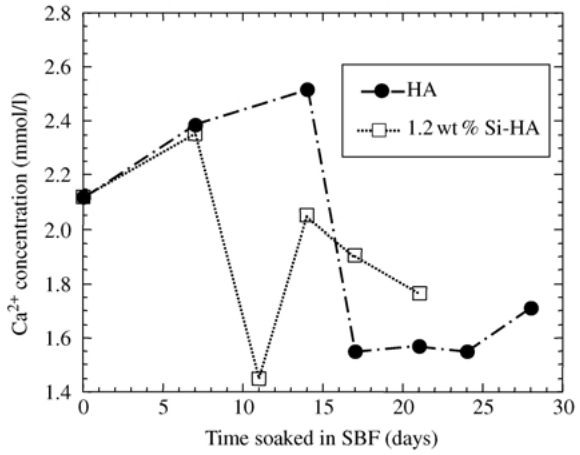

Figure 4 Calcium ion concentration (mmol/l) in SBF soaking solution.

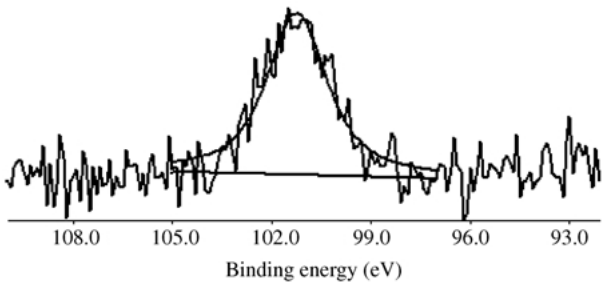

Figure 6 XPS spectra of 1.2 wt % Si–HA.

Discussion and conclusion

Analysis of the HA and Si–HA compositions produced for this study using XRD and FTIR confirmed the proposed mechanism of silicon (or silicate) substituting for phosphorus (or phosphate), in accordance with the results reported previously [12]. The analysis by XPS, however, has been able to confirm conclusively that the silicon does exist as a tetrahedral silicate, SiO_4 group, rather than in a polymeric or SiO_2 form. This important finding supports the analogy between silicon, or silicate substitution with the well-characterized carbonate substitution of phosphate groups in hydroxyapatite [10].

The displacement observed in the zeta potential curves is attributed to the substitution of some PO_4^{3-} groups by SiO_4^{4-} groups that occurred in the Si–HA material, which can be explained by the mechanism of substitution showed in Equation 2.

$$10Ca^{2+} + (6-x)\ PO_4^{3-} + SiO_4^{4-}x + (2-x)\ OH^- \rightarrow Ca_{10}(PO_4)_{6-x}(SiO_4)_x(OH)_{2-x} \quad (2)$$

In fact, it is known that PO_4^{3-} groups are preferentially located at HA surfaces [28] and therefore the substitution of these ions for SiO_4^{4-} groups should result in a decrease in surface charge, as indicated by zeta potential measurements. The decrease in intensity of the peak in the FTIR spectra that corresponds to the OH^- group on the Si–HA was expected since according to the mechanism of Equation 2 the substitution of the phosphate group for the silicate group leads to some OH^- loss in order to maintain the charge balance.

FTIR and XPS results clearly support the substitution mechanism of Equation 2 for Si–HA. Vibrational wavelength of 888 and 504 cm^{-1} indicate the presence of SiO_4 and the binding energy of silicon at 101 eV corresponds to (Si–O) bonding [27].

To complement the above-mentioned interpretation, zeta potential results indicate the shifting of the zeta potential of Si–HA towards negative values compared to unmodified HA. Literature reveals that PO_4^{3-} seem to be preferentially located at surface of HA [28], which may somehow contribute to the lower Ca/P $\approx$ 1.4 observed under XPS analysis when compared to the stoichiometric value of Ca/P $\approx$ 1.67 since under this technique only around the first nanometers are analyzed.

Soaking the HA and the 1.2 wt % Si–HA samples in a simulated body fluid produced comparable trends, but differed in the time scale of the events. In particular, the Si–HA changed from a dissolution behavior (increased ion concentration in the SBF solution) to a surface precipitation behavior (a decrease in ion concentration in the SBF solution) in less time than the HA sample. This result may be due to a greater solubility of the Si–HA material, leading to a faster super-saturation of the SBF solution and therefore a faster precipitation of an apatite layer from the super-saturated SBF. The data in Figs. 4 and 5 do, however, suggest that the Ca^{2+} and PO_4^{3-} ion concentrations of the SBF solutions from the HA and Si–HA samples were comparable at 7 days, which is the measured time point before apatite layer formation occurred with the Si–HA. The surface properties of the HA and Si–HA ceramics may therefore have controlled the time scale for the change from dissolution to apatite precipitation. The results in this study show that the surface charge/zeta potential of the two materials were significantly different at pH = 7.4. The more electronegative Si–HA surface may provide a preferential site for the nucleation of an amorphous calcium phosphate apatite layer than the HA surface. This could occur via the adsorption of Ca^{2+} ions on to the electronegative surface, resulting in an increase in surface charge and the attraction of phosphate groups. The effect of the real-time formation of an apatite layer on the surface charge of Si–HA and HA will be studied in the future.

Due to the low dissolution rate of the materials under study, a higher amount of silicon was incorporated in the material to be analyzed (1.2 wt % Si) in the dissolution testing. No compositional modification was detected for HA before and after dissolution, as shown in Table I. However, preferential ionic release of silicon was observed for Si–HA. Previous results showed that the silicon substitution caused a substantial increase in distortion index of the phosphate groups in HA and a decrease in the number OH^- groups [29]. It is possible that these lattice disturbances/distortions by silicon incorporation may lead to a higher susceptibility of SiO_4^{4-} release from the HA structure.

Acknowledgment

The authors wish to acknowledge the financial support of ref. SFRH/BD/6173 grant financed by FCT (Fundação para a Ciência e Tecnologia).

References

1. E. M. CARLISLE, *Fed. Proc.* **43** (1984) 680.
2. E. M. CARLISLE, in ''Silicon Biochemistry'', edited by D. Evered and M. O'Connor (Wiley, New York, 1986).
3. K. SCHWARZ, in ''Biochemistry of Silicon and Related Problems'', edited by G. Bendz and I. Lindqvist (Plenum Press, New York, 1978) pp. 207–230.
4. K. SCHWARZ and D. B. MILNE, *Nature* **239** (1972) 333.
5. M. G. VORONKOV, V. I. SKOROBOGATOVA, E. K. VUGMEISTER and V. MAKARSKII, *Dok/ady Biochemistry* **222** (1975) 29.
6. L. L. HENCH, in ''Biological Implications'' (1999) pp. 116–163.
7. P. E. KEETING, M. J. OURSLER, K. E. WEIGAND, S. K. BONDS, T. S. SPELSBERG and B. L. RIGGS, *J. Bone Minera/ Res.* **7** (1992) 1281.
8. L. L. HENCH, *J. Phys.* **43** (1982) 625.
9. L. L. HENCH, *J. Am. Ceram. Soc.* **74** (1991) 1487.
10. L. L. HENCH and J. WILSON, ''An Introduction to Bioceramics'' (World Scientific Publishing Co., Singapore, 1999).
11. L. J. JHA, S. BEST, J. D. SANTOS, I. R. GIBSON and W. BONFIELD, ''Silicon-Substituted Apatites and Process for the Preparation Thereof'', Worldwide Patent, PCT/GB97/02325 and US Patent Serial No 09/147773 (1999).
12. I. R. GIBSON, S. M. BEST and W. BONFIELD, *J. Biomed. Mat. Res.* **44** (1999) 422.
13. I. R. GIBSON, J. HUANG, S. M. BEST and W. BONFIELD, in ''Bioceramics, Vol. 12, Proceedings of the 12th International Symposium on Ceramics in Medicine (Nara, Japan November 1999)'', edited by H. Ohgushi, G. W. Hastings and T. Yoshikawa (World Scientific Publishing Co., London, 1999) pp. 191–194.
14. I. R. GIBSON, K. A. HING, P. A. REVELL, J. D. SANTOS, S. M. BEST and W. BONFIELD, *Key Engin. Mat.* **218–222** (2002) 203.
15. N. G. MAROUDAS, *J. Theoret. Biol.* **49** (1975) 417.

16. P. B. VAN WACHEM, A. H. HOGT and T. BEUELING *et al*., *Biomaterials* **8** (1987) 323.
17. J. E. DAVIES, in ''Surface Characterization of Biomaterials'', edited by B. D. Ratner (Elsevier, Amsterdam, 1998) pp. 219–234.
18. R. M. SHELTON, A. C. RASMUSSEN and J. E. DAVIES, *Biomaterials* **9** (1988) 24.
19. P. DUCHEYNE, J. BEIGHT, J. CUCKLER, B. EVANS and S. RADIN, *ibid*. **11** (1990) 531.
20. H. OHGUSHI, V. M. GOLDBERG and A. I. CAPLAN, *J. Orthop. Res*. **7** (1989) 568.
21. G. DACULSI, R. Z. LE GEROS, E. NERY, K. LYNCH and B. KEREBEL, *J. Biomed. Mater. Res*. **23** (1989) 883.
22. K. HYAKUNA, T. YAMAMURO, Y. KOTOURA, Y. KAKUTANI, T. KITSUGI, H. TAKAGI, M. OKA and T. KOKUBO, *ibid*. **23** (1989) 1049.
23. Y. KOTOURA, T. YAMAMURO, J. SHIKATA, Y. KAKUTANI, T. KITSUGI, K. HYAKUNA and H. TANAKA, *Orthop. Res. Sci*. **13** (1986) 633.
24. T. FUJIU and M. OGINO, *J. Biomed. Mater. Res*. **18** (1984) 845.
25. I. REHMAN and W. BONFIELD, *J. Mat. Sci.: Mater. in Med*. **8** (1997) 1.
26. R. A. NYQUIST, C. L. PUTZIG and M. A. LEUGERS, *Infrared and Raman Spectral Atlas of Inorganic Compounds and Organic Salts* **3** (1995).
27. NIST – National Institute of Standards and Technology Database.
28. W. VAN RAEMDONCK, P. DUCHEYNE and P. De MEESTER, *Metal and Ceramic Biomaterials* (CRC Press, 1984) 143–146.
29. I. R. GIBSON, L. J. JHA, J. D. SANTOS, S. M. BEST and W. BONFIELD, in ''Bioceramics, Vol. 11, Proceedings of the 11th International Symposium on Ceramics in Medicine (New York, NY, USA, November 1998)'', edited by R. Z. LeGeros and J. P. LeGeros (World Scientific Publishing Co., USA, 1998).

Received 24 May
and accepted 29 May 2002